RSC Pharmaceutics

ROYAL SOCIETY OF CHEMISTRY

PAPER

View Article Online
View Journal | View Issue

Cite this: *RSC Pharm.*, 2025, **2**, 114

A novel solid formulation of a rivaroxaban eutectic using a hot melt extruder with improved thermal stability and dissolution profile†

Parth S. Shaligram,[a,b] Ranjitsinh Pawar,[c] Nagabhushan Shet[a,c] and Rajesh G. Gonnade *[a,b]

The current work aims to enhance the solubility, dissolution rate and stability of the poorly water-soluble drug rivaroxaban (RXB) by preparing an amorphous solid dispersion (ASD) of its eutectic with mandelic acid (MA) as an acidic coformer. Eutectics generally have lower melting points compared to their constituents. Hence, they can be used to lower the processing temperature of the drug to prevent its thermal degradation under a hot melt extruder (HME). Six eutectics of RXB were prepared with various carboxylic acid coformers. The eutectic of RXB and MA (1 : 4, mol/mol), which had the lowest melting point, was selected for the HME process. A hydrophilic polymeric matrix was used to prepare the ASD of the selected eutectic. The resultant extruded filament was further subjected to solubility and dissolution studies. We could load up to 25% RXB–MA eutectic in the polymer matrix to yield a complete ASD of RXB–MA at a lower processing temperature of 110 °C. The ASD of the RXB–MA eutectic showed three times the drug release compared to pure RXB. The RXB–MA (1 : 4) eutectic lowered the HME process temperature, further enhancing the thermal stability, solubility and dissolution rate of RXB. The solubility and dissolution rate enhancement might favourably impact the drug's bioavailability.

Received 1st September 2024,
Accepted 3rd November 2024

DOI: 10.1039/d4pm00253a

rsc.li/RSCPharma

Introduction

Rivaroxaban ((*S*)-5-chloro-*N*-({2-oxo-3-[4-(3-oxomorpholin-4-yl) phen-yl] oxazolidin-5-yl}methyl)thiophene-2-carboxamide) (Fig. 1) is a selective and highly potent factor Xa inhibitor used orally as an anticoagulant.[1,2] Factor Xa inhibitors block the generation of thrombin, which reduces thrombin-mediated coagulation. RXB prevents thromboembolism after hip or knee replacement surgery.[3,4] RXB is also used with many chemotherapeutic agents.[5] The marketed formulation of RXB is the Xarelto® tablet with oral dosages of 10 mg, 15 mg and 20 mg potencies. As per the market value, it was reported that RXB's market size was USD 14.89 million in 2022. The global RXB market will reach USD 25.59 million in 2030, growing at a CAGR (Compound Annual Growth Rate) of 7% (Global Rivaroxaban Market-Industry Trends and Forecast to 2030). The patent WO2007039132 has reported the crystalline forms I, II and III, the amorphous form, the hydrate, the NMP solvate and the THF clathrate of RXB. It is classified as a Biopharmaceutical Classification System Class II (BCS Class II) drug and possesses low solubility in aqueous solutions, affecting its bioavailability.[6] Moreover, it is practically insoluble in most industrial solvents,

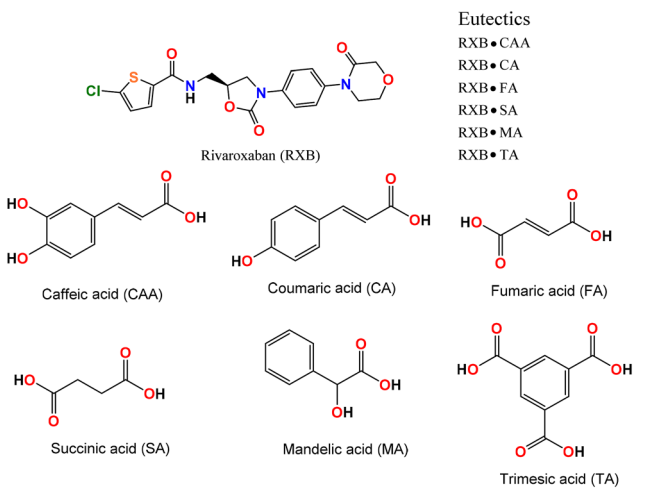

Fig. 1 Molecular structure of rivaroxaban (RXB) and coformers used for eutectic preparation.

[a]*Physical and Materials Chemistry Division, CSIR-National Chemical Laboratory, Dr Homi Bhabha Road, Pashan, Pune 411008, India. E-mail: rg.gonnade@ncl.res.in*
[b]*Academy of Scientific and Innovative Research (AcSIR), Sector 19, Kamla Nehru Nagar, Ghaziabad, Uttar Pradesh, 201002, India*
[c]*Bharati Vidyapeeth Deemed to be University, Poona College of Pharmacy, Department of Pharmaceutics, Erandwane, Pune 411 038, Maharashtra, India*

†Electronic supplementary information (ESI) available: DSC, TGA, PXRD, and FTIR data for the individual components, eutectics, and eutectic ASD. See DOI: https://doi.org/10.1039/d4pm00253a

such as ethanol, methanol, isopropyl alcohol, *etc*. Therefore, formulation scientists worldwide are working to tackle the problems of aqueous solubility, which would further improve its bioavailability. Efforts have been made to develop alternative crystalline phases of RXB to enhance its physicochemical properties, which might positively impact its therapeutic efficacy. The novel solid formulation includes cocrystals, nano-formulations, microemulsions, liposomes, nanosuspensions, solid dispersions, cyclodextrin inclusions, *etc*.[7–13] The improvement in physicochemical and biopharmaceutical properties might augment therapeutic efficacy. Formulating ASDs of poorly water-soluble active pharmaceutical ingredients (APIs) can be the way to deal with solubility problems.

Hot melt extrusion (HME) is widely used in the pharmaceutical industry to prepare amorphous solid dispersions (ASDs).[14] The amorphous form of APIs is considered "Latter-generation solid dispersions",[15] wherein the amorphous form of the drug shows higher dissolution rates. The other methods of preparing ASDs include solvent evaporation, freeze drying, supercritical fluid processing, spray drying and thermal melting.[16–20] Compared to these traditional preparation methods for ASDs, HME is the most promising solvent-free, continuous, industry-feasible and scalable process for preparing ASDs.[21] There have been several attempts to prepare polymeric amorphous solid dispersions (ASDs) containing RXB to improve its physicochemical properties.[22,23] APIs must be dissolved or melted into a polymeric matrix to prepare an ASD using the extrusion technique. This process requires a temperature high enough to melt the drug and the polymer. However, many drugs have a high melting point or heat-labile properties. It is a major challenge for the formulator to improve the chemical stability of such drugs having heat sensitivity problems. Researchers have tried different ways to overcome the thermal instability of thermo-sensitive APIs. For example, the thermal degradation of meloxicam could be avoided by choosing a suitable polymer, optimizing extrusion parameters and introducing alkaline substances in the formulation.[24] Also, screw design improvement and optimized process conditions in the HME technique can improve mixing and reduce the residence time of APIs at higher temperatures.[24,25]

Eutectics are a mixture of two or more components that usually do not interact to form a new chemical compound but, at certain ratios, inhibit the crystallization process of one another, resulting in a solid system having a lower melting point than the constituents.[15,26–28] A eutectic is defined based on its low melting point compared to the individual components. Eutectics have more free energy and show enhanced solubility, dissolution rate and bioavailability of poorly water-soluble drugs.[15,29] Our group formulated and reported a detailed study of six eutectics of RXB with different acidic coformers, namely caffeic acid (CAA), coumaric acid (CA), fumaric acid (FA), succinic acid (SA), mandelic acid (MA) and trimesic acid (TA).[29] Eutectics of RXB with CAA, CA, and FA coformers showed enhanced solubility, dissolution rate, and bioavailability. The prepared eutectics were characterized using powder X-ray diffraction (PXRD), differential scanning calorimetry (DSC), hot stage microscopy (HSM) and infrared spectroscopy (IR).[29,30]

Out of the six eutectics, RXB–MA (1 : 4, mol/mol) was selected to prepare an ASD using the hot melt extrusion technique. This particular eutectic showed a maximum reduction in the melting point from a high RXB (231.5 °C) to a low RXB–MA eutectic (103.2 °C). The degradation of RXB can be efficiently prevented by lowering the melting point and extrusion temperature. Hydrophilic polymers, namely Kollidon® VA 64 and plasticizer Kolliphor® P 188, were used as a polymeric matrix to formulate the ASD. The effect of the eutectic and hydrophilic polymer on the solubility and the dissolution profile of RXB was later analyzed by solubility and powder dissolution studies. The eutectic and extruded filament was found to be stable during the entire period of stability studies. This study will provide a new way to achieve thermal stability of thermally sensitive APIs by preparing their eutectics for formulating ASDs using a hot melt extruder.

Experimental

Materials and methods

RXB was a generous gift from Alkem Pharma, India. Mandelic acid was purchased from Aldrich Chemistry, Mumbai. Kollidon® VA 64 and Kolliphor® P 188 were generous gifts from BASF Corporation (Mumbai, India). HPMC E5 and HPMC E15 were received as gift samples from Colorcon (Mumbai, India). Distilled water was generated using a Millipore Direct-Q ultra-pure water system (Merck Millipore, India).

Preparation of the RXB–MA eutectic

The RXB–MA eutectic was developed by grinding equimolar concentrations of RXB and MA using a mortar and a pestle in the presence of an ethanol–acetone (1 : 1 v/v) solvent system. During the liquid-assisted grinding (LAG) method, the solvent or solvent system acts as a catalyst and/or a lubricant.[31] The mortar and pestle generated the energy required to cause the intermolecular interaction between RXB and MA. The resultant compound was subjected to further analysis.[29]

Binary phase diagram

The phase diagram of the RXB–MA eutectic with varying mole fractions was plotted to confirm the exact molar ratio required to form a eutectic. Mixtures of varying mole fractions from 1 : 1 to 1 : 9 (RXB : MA) were prepared by grinding the sample using a mortar and a pestle. DSC analysis of all the mixtures of RXB and MA was performed to estimate their melting temperature.[29]

Differential scanning calorimetry (DSC) analysis

DSC studies of RXB, MA and the RXB–MA (1 : 4) eutectic and milled extruded filaments were carried out using the Mettler Toledo DSC 822e instrument (London, United Kingdom). 3 mg powder samples were weighed accurately and placed into an

aluminium crucible. An empty pan with a locked lid was placed as a reference. The sample was heated from 25 °C to 250 °C at a heating rate of 10 °C min^{-1} to improve the observation accuracy for all the thermal events.[32] The analysis was carried out under an inert environment of nitrogen gas with a flow rate of 40 mL min^{-1}.[29]

Powder X-ray diffraction (PXRD) analysis

PXRD data of powder samples were recorded on multiple systems. PXRD of eutectic samples was carried out using an X'Pert PRO diffractometer system (PANalytical, Almelo, Netherlands) with CuKα radiation. The tube voltage and current were set at 45 kV and 40 mA, respectively. The divergence slit and anti-scattering slit settings were set at 0.48° for the 10 mm sample size diffraction experiment. Powdered samples of RXB, MA and the RXB–MA eutectic were analyzed using the PXRD technique. Each sample was placed on a sample holder and continuously scanned between 3.5° and 50° 2θ with a step size of 0.017° and a step time of 25 s per step.[33] The experimental PXRD profiles of individual excipients used in the HME and all the final batches were recorded on an ARL EQUINOX 100 (Thermo Scientific, USA) PXRD machine with Cu Kα radiation. The tube voltage and current were set at 40 kV and 0.8 mA, respectively. Each sample was placed on a sample holder and scanned from 3° to 100° 2θ values using a stationary detector. The experimental PXRD patterns were refined using X'PertHighScore software.

Fourier transform infrared spectroscopy (FTIR)

FTIR spectroscopy was carried out on a JASCO FT/IR-4100 Fourier Transform Infrared Spectrometer (JASCO, Japan). FTIR analysis of RXB, MA and the RXB–MA eutectic was performed in KBr transmittance mode (with a sample concentration of 2 mg in 20 mg of KBr). Scans were recorded over the range of 4000–400 cm^{-1} with a resolution of 4 cm^{-1}. Data were analyzed using Spectra Manager software (JASCO).[29]

Hot stage microscopy (HSM) analysis

HSM of the RXB–MA (1 : 4) eutectic was performed on Linkam Scientific Instruments Ltd (Tadworth, England), equipped with an EHEIM Professional4+ temperature controller and an optical microscope (Leica S8APO) with a Q imaging camera to capture the images. The sample was focused under the microscope at 10× zoom. The photos were acquired after specific intervals during the heating process, wherein the samples were heated from 50 °C to 250 °C at 5 °C min^{-1}.[29]

High-performance liquid chromatography (HPLC)

The concentration of RXB was determined using a Waters 515 HPLC system (Waters Corporation, Milford, MA, USA), which was attached to a reversed-phase column (250 × 4.6 mm; 5 μm; C18). Analyte detection was done at a wavelength of 249 nm with the help of a PDA detector. An acetonitrile : water (55 : 45 v/v) mobile phase was selected for the analysis.[34] The flow rate of the mobile phase was fixed at 1.2 mL min^{-1}. The retention time of RXB was set at 3.2–3.4 min with an injection volume of 5 μL.

Thermogravimetric analysis (TGA)

TGA of RXB was performed to analyze the thermal stability of RXB using an STA 6000 Simultaneous Thermal Analyzer (PerkinElmer, Waltham, MA, USA). About 5–10 mg of RXB powder was weighed into an alumina crucible. The sample was heated up to 500 °C at a 10 °C min^{-1} heating rate. Air was purged at a 19.8 mL min^{-1} rate, and the percent (%) weight loss was monitored. The temperature *vs.* percent (%) weight graph was plotted using Pyris Manager software.

Thermal degradation study by HPLC

Powder samples of RXB were heated and held constant for 5 minutes at various temperatures using Linkam Scientific Instruments Ltd (Tadworth, England). The main motive to conduct this study was to understand the effect of temperature on the thermal stability of RXB during 5 minutes of the HME process. It took around 5 minutes to complete the HME process at a screw speed of 100 rpm. After heating, the resultant powder samples were dissolved in appropriate solvents for HPLC analysis.[35]

HME process

A micro-conical co-rotating twin screw extruder, the HAAKE MiniCTW extruder (Thermo Scientific, Karlsruhe, Germany), was utilized for the hot melt extrusion process. RXB or the RXB–MA eutectic and excipients were accurately weighed to make a total batch of 5 g. These powders were placed in a Retsch MM 400 ball mill for uniform mixing at 20 Hz for 3 min. The resultant physical mixture was then manually fed into the extrusion machine. The extrusion process was carried out at varying temperatures, and the screw speed was adjusted to 100 rpm. The extruded filament was then cooled to room temperature. For further analysis, the filament was crushed to powder using a Retsch MM 400 ball mill.

Scanning electron microscopy (SEM)

An SEM (NOVA NANOSEM 450, FEI, Netherlands) equipped with a backscattered electron detector (BSE) was used to visualize the optimized formulation's extruded filament and powdered samples of RXB, RXB–MA (1 : 4) eutectic and RXB–MA ASD. BSE images were collected at an acceleration voltage of 20 kV. All samples were attached to double-sided carbon tape on aluminium stubs. The radiation of plasma gold beams was targeted on aluminium stubs for the coating with a layer of 5 nm thickness for about 60 seconds.

Saturation solubility

Saturation solubility was determined by adding an excess amount of RXB, RXB–MA eutectic and optimized HME batch powder samples into a beaker full of distilled water. The solution was stirred for 24 hours at room temperature. An IKA RCT 5 digital magnetic stirrer (IKA Pvt. Ltd, Bengaluru, India) was used to maintain a constant stirring rate of 500 rpm. The concentration of RXB in distilled water after stirring for 24 h was analyzed using the HPLC method described above.

Dissolution study

In vitro drug release studies were carried out for RXB, RXB–MA eutectic, milled and powdered filaments of an optimized batch and the RXB marketed formulation with a dissolution tester DS 8000+ (Labindia, Mumbai) along with a syringe pump. The dissolution studies were carried out in distilled water as RXB shows pH independent solubility. A dissolution study was performed on a 15 mg powder sample of RXB, RXB–MA eutectic (equivalent to 15 mg of RXB), the milled filament of the optimized batch (equivalent to 15 mg of RXB) and the RXB marketed formulation (15 mg), as per the IP specification, with USP type II (paddle) apparatus at 37 ± 0.5 °C with a paddle rotating speed of 50 rpm. The dissolution medium was 900 mL of distilled water. Automatic sampling was set to withdraw 5 mL of aliquots at 5, 10, 15, 30, 45 and 60 minutes. The samples were analyzed after required dilutions using the HPLC method discussed earlier.

Stability study

Accelerated and long-term stability studies were performed for eutectics for six months and twelve months, respectively,[29] whereas a three-month accelerated study was carried out for the final batch of HME filaments. Stability studies were performed in a stability chamber (Thermolab Scientific Instruments, Mumbai, India). For accelerated stability studies, the temperature and relative humidity were respectively set at 40 ± 2 °C and 75 ± 2%.[27,33] The temperature and relative humidity were set at 30 ± 2 °C and 65 ± 5%, respectively, for long-term stability studies. The samples were collected and tested using DSC and PXRD techniques.

Results and discussion

Preparation and characterization of eutectics

RXB is a BCS class II drug with pH-independent solubility in water (5–7 mg L^{-1}).[3] We started our research work to improve the solubility of RXB by developing its multicomponent solids. Our attempts to develop multicomponent solids of RXB resulted in the formation of six eutectics with different acidic coformers.[29] The RXB–MA eutectic melted at the lowest temperature amongst all the six eutectics. Therefore, further characterization studies were performed on the RXB–MA eutectic.

Binary phase diagram

The construction of a phase diagram is essential for understanding the exact composition of the drug and coformer in the eutectic. Solidus and liquidus curves were constructed from the melting temperatures of the binary mixtures in varying molar ratios using DSC studies. The phase diagram revealed the experimental eutectic point of the binary mixture to be at a 0.2 : 0.8 molar ratio of RXB–MA (Fig. 2). Except for 0.2 : 0.8 (RXB–MA), all the other ratios of mixtures showed two endothermic events.[29,36] Hence, preparing the RXB–MA eutectic in a 1 : 4 molar ratio was necessary.

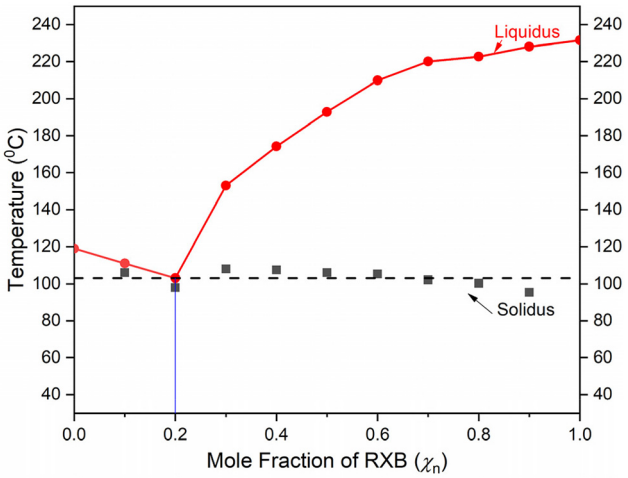

Fig. 2 Phase diagram study of RXB–MA. Mole fraction of RXB *vs.* temperature plot indicates the eutectic point at a ratio of 0.2 : 0.8, *i.e.*, 1 : 4.

Differential scanning calorimetry (DSC) analysis

DSC analysis was performed on the RXB–MA (1 : 4) mixture to confirm the eutectic formation and to observe any phase transitions during the heating process. Fig. 3 presents the DSC thermograms of RXB, MA and RXB–MA. The RXB–MA eutectic showed a single endotherm centred at 103.2 °C, which was attributed to its melting. The endotherm showed an evident fall in melting temperature compared to the pristine RXB and MA, confirming that the mixture is eutectic.[29,37]

Hot stage microscopy (HSM) analysis

Furthermore, an HSM study of the RXB–MA (1 : 4) eutectic was performed to confirm the congruent melting of the eutectic. At 103 °C, the eutectic melted completely without leaving any traces of RXB or MA (Fig. 4).[29] The HSM images showed the sharp melting of the mixture, which means that the crystalline

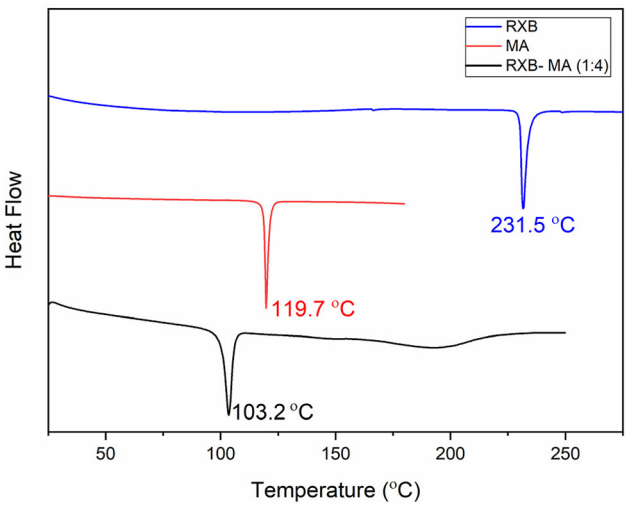

Fig. 3 DSC thermograms of RXB, MA and RXB–MA (1 : 4) eutectic.

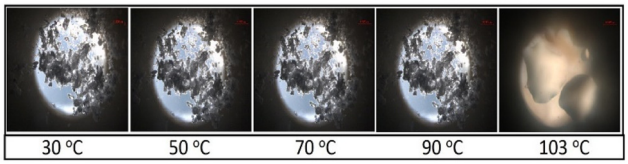

Fig. 4 HSM images of the RXB–MA (1 : 4) eutectic at different time intervals.

nature of both the individual moieties in the mixture is not hampered throughout the preparation.[38]

Powder X-ray diffraction (PXRD) studies

The diffractogram of the eutectic was examined thoroughly and compared to the diffractograms of RXB and MA. Fig. 5 presents the PXRD patterns of RXB, MA and the RXB–MA (1 : 4) eutectic. The characteristic diffraction peaks of RXB, MA and the RXB–MA eutectic are mentioned in Table S9 (ESI†). The PXRD pattern of the RXB–MA eutectic revealed that it contained all the diffraction peaks of RXB and MA. This contrasts the PXRD profile of cocrystals/salts, which has entirely new diffraction peaks. Cocrystals and molecular salts are homogeneous monophasic entities containing all the neutral components in a stoichiometric molar ratio. The diffractograms of cocrystals and salts are exclusively different from those of their components.[39] The PXRD patterns of RXB–MA revealed diffraction peaks for RXB, indicating the formation of eutectics.

Fourier transform infrared (FTIR) spectroscopy studies

The FTIR spectrum of RXB (Fig. 6) showed characteristic bands at 3366 cm^{-1} for the amine group, 1737 cm^{-1} for the –C═O group and 832 cm^{-1} for the C–Cl group. MA showed characteristic peaks at 1431 cm^{-1} for –OH bending in carboxylic acid and 1717 cm^{-1} for C═O stretching in the carboxylic acid group, and the –OH peak was observed to be merged. The FTIR vibrational frequencies for the RXB–MA (1 : 4) eutectic appeared at 3367 cm^{-1}, 1717 cm^{-1}, 835 cm^{-1}, 1432 cm^{-1}, and 1717.5 cm^{-1}, showing a slight shift in the vibrational frequencies concerning the individual components. The –OH peak was observed to have merged with the amine peak. Thus, from FTIR studies, it was noticed that there was a very subtle shift in the vibrational frequencies, which was too small even to consider. Therefore, it helped to conclude that there was hardly any change in the identity of individual components of the eutectic. The FTIR spectra of the RXB–MA eutectic confirmed the presence of all the vibrational frequencies present in the individual components. This confirmed no chemical interaction between the RXB and MA, which supports the results of DSC and PXRD studies regarding the formation of eutectics.[29]

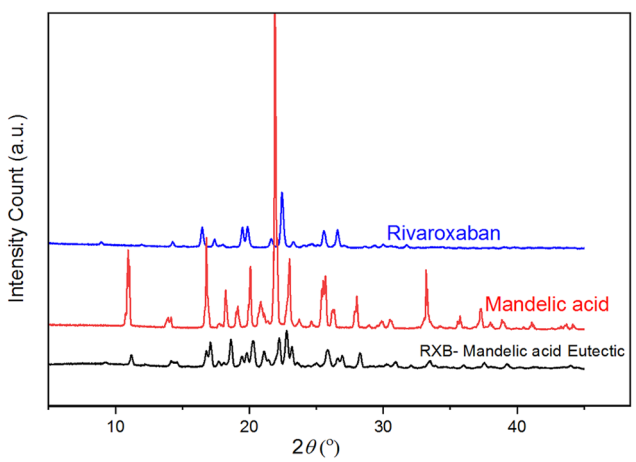

Fig. 5 PXRD profiles of RXB, MA and the RXB–MA eutectic mixture.

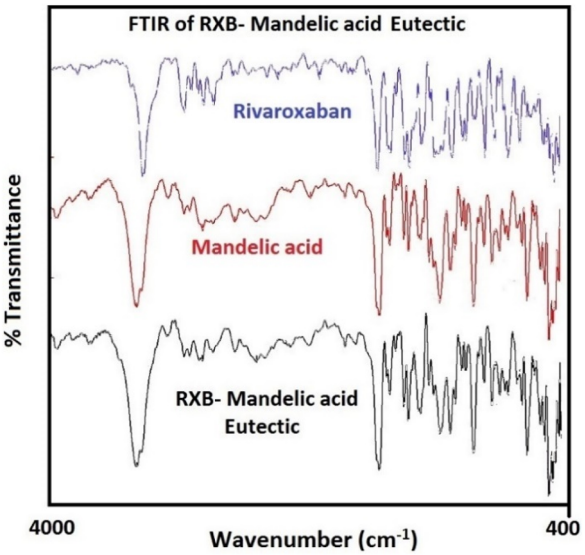

Fig. 6 The FTIR spectra of RXB, MA and the RXB–MA eutectic.

Stability study of the RXB–MA (1 : 4) eutectic

Due to their high free energy, poor stability is the main challenge associated with eutectic mixtures. Therefore, the RXB–MA (1 : 4) eutectic was subjected to accelerated (40 ± 2 °C and 75% RH ± 2% for 6 months) and long-term stability studies (30 ± 2 °C and 60% ± 5% RH for 12 months). After six months of accelerated stability study, the DSC thermograms recorded for the eutectics were similar to the DSC thermograms recorded for the freshly prepared eutectics (ESI, Fig. S1†). The long-term stability of the eutectics was checked using the DSC and PXRD techniques, which revealed high stability and no change in the crystal phases upon storage for all the eutectics (ESI, Fig. S1 and S2†).

Thermal degradation of RXB

Thermal degradation of RXB was studied by both TGA and HPLC.[35] Fig. 7 shows the TGA graph of RXB (black curve). TGA revealed no significant weight loss of RXB up to its melting temperature. At 231.5 °C, only 0.61% weight loss for RXB was estimated. Furthermore, drastic weight loss of RXB was

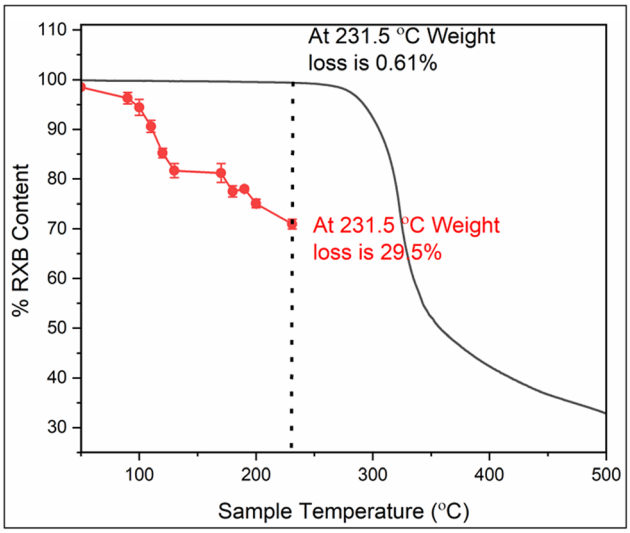

Fig. 7 TGA profile (black curve) of RXB at a heating rate of 10 °C min^{-1}. The red curve represents the thermal degradation of RXB measured by HPLC after heating for 5 min on the hot stage. The dotted line represents the melting point of RXB.

observed above its melting temperature, indicating sudden thermal degradation of RXB.

The thermal degradation behavior of RXB during the HME process was studied using controlled heating of pure RXB and analyzed through HPLC. Fig. 7 presents the thermal degradation plot of RXB when heated and held for 5 minutes at various temperatures starting from 40 °C to 231 °C (red curve). RXB powder was observed to be comparatively stable below 110 °C with approximately 10% degradation due to heat. From temperature 180 °C to 231.52 °C, up to 30% of RXB was degraded. This suggested that the HME process for RXB should be conducted at lower temperatures ranging up to 110 °C. Therefore, the RXB–MA eutectic, having a melting point of 103.2 °C, was selected for the HME process.

Optimization of the HME process

Different hydrophilic polymers were screened for the preparation of ASDs. Different trial batches of HME were prepared with RXB and polymers, namely HPMC E5, HPMC E15 and Kollidon® VA 64. The DSC thermograms of extruded filaments using HPMC E5 and HPMC E15 with 10% RXB showed small humps in the temperature range of 200 °C–220 °C. Such irregularity and humps were absent in the case of the DSC thermogram of the extrusion batch of Kollidon® VA 64 with 10% RXB (ESI, Fig. S3†). For further evaluation of the drug–polymer compatibility, FTIR studies were carried out on the polymer, plasticizer and the physical mixture of all the components in the ASD. It was found that the prominent bands at 3366 cm^{-1} and 1737 cm^{-1} of RXB were found in the FTIR spectrum of the physical mixture. On the other hand, the FTIR spectrum of the formulated ASD contained only the prominent frequencies of the polymer and plasticizer. This suggested that Kollidon® VA 64 was compatible to be used with RXB (ESI, Fig. S4†). Hence, Kollidon® VA 64 was a suitable hydrophilic polymer with RXB for preparing HME batches.[23]

Generally, the polymer–plasticizer combination is used as a polymeric matrix in HME batches to prepare ASDs.[40,41] Also, plasticizers are known to reduce the glass transition temperature (T_g) and melt viscosity of the polymers. Therefore, for trial HME batches, Kollidon® VA 64 and Kolliphor® P 188 (plasticizer) with a 10% RXB load were used. The rpm of the twin screw was set at 100 for all the batches since a screw speed below 100 rpm caused an increase in the blend's residential time, resulting in the production of discoloured filaments that suggested the initiation of degradation. At 100 rpm, a uniform filament with a smooth surface was obtained. At a higher rpm, it was observed that the extruded filaments had hard and rough surfaces with non-uniform thickness.[24,25] By considering factors such as the melting point of RXB (231.52 °C), processing conditions (shear stress due to screws) and the use of polymers, we initiated the extrusion at 200 °C. After the extrusion at 200 °C, a blackish fragmented extruded filament was obtained. Discolouration or a change in colour towards a blackish shade generally suggests that the components from the extruded filament are degraded.[42] Therefore, TGA of Kollidon® VA 64 was performed to monitor its thermal stability (ESI, Fig. S5†). It was found that the higher processing temperatures were found to be unsuitable as RXB and the polymer showed thermal degradation around 200 °C. It was also found that lowering the temperature to 190 °C and 180 °C resulted in the formation of brownish and yellowish extruded filaments, respectively (Fig. 8). The trend in the colour change also confirmed that discolouration reduces as the temperature is lowered while processing. These observations, along with the previously mentioned thermal degradation study of RXB using the HPLC method, simulating the HME processing conditions, strongly suggest that a lower processing temperature is required. Hence, to avoid excessive thermal degradation of

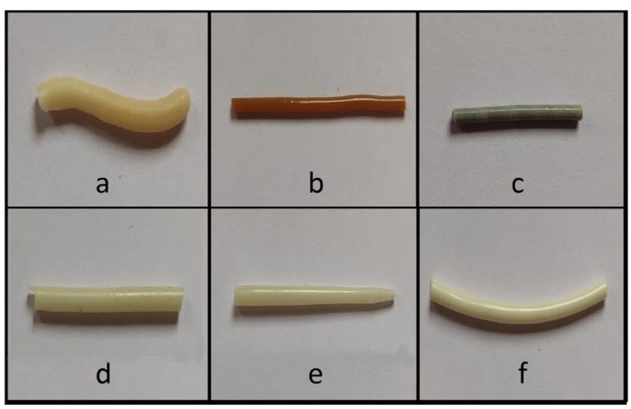

Fig. 8 Hot melt extrusion batches with a screw speed of 100 rpm at different temperatures: (a) filament of batch B1 with 10% RXB at 180 °C, (b) filament of batch B2 with 10% RXB at 190 °C, (c) filament of batch B3 with 10% RXB at 200 °C, (d) filament of batch B4 with 10% RXB–MA at 90 °C, (e) filament of batch B5 with 10% RXB–MA at 100 °C and (f) filament of batch B6 with 10% RXB–MA at 110 °C.

RXB, extrusion should be conducted in the temperature range of 90–110 °C.

A total of 10% RXB–MA (1 : 4) eutectic with the polymeric combination was extruded at different temperatures, *i.e.*, 90 °C (B4), 100 °C (B5), and 110 °C (B6). Among the three batches, the filament of batch B6 showed the best appearance with a shiny, uniform white extrudate, whereas other batches (B4 and B5) had a rough and non-uniform surface (Fig. 8). All these batches were further analyzed using DSC and PXRD studies. Fig. 9 presents individual DSC endotherms of batches B4, B5 and B6. Batches B4 and B5 show different thermal events in the DSC curve, which might be due to incomplete amorphization. On the other hand, such patterns were absent in the DSC endotherm of batch B6. In the case of batches B4 and B5, a very small but visible hump was observed near the eutectic point (100 °C to 110 °C), whereas for batch B6, no such endothermic hump was observed. Also, a small and blunt endotherm was observed in batches B4 and B5 at around 50 °C, which might be congruent to the sharp endotherm of Kolliphor® P 188 at 53.19 °C (ESI, Fig. S6a and S6b†). On the other hand, it was evident that Kolliphor® P 188 was completely miscible in the Kollidon® VA 64 polymeric matrix in batch B6. This suggests that in batch B6, the eutectic was completely incorporated into the polymeric matrix.

As we discussed earlier, batch B6 was extruded at 110 °C. Also, the glass transition temperature of Kollidon® VA 64 was observed near 142 °C. The glass transition temperature of Kollidon® VA 64 was further reduced to approximately 105 °C after the addition of Kolliphor® P 188 (ESI, Fig. S6b†). Therefore, complete amorphization of the RXB–MA (1 : 4) eutectic (103.2 °C) could happen at a processing temperature of 110 °C.

Fig. 10 shows PXRD diffraction patterns of B4, B5 and B6, along with diffraction patterns of Kolliphor® P 188 and the sample holder. Intense peaks of plasticizer Kolliphor® P 188 were obtained at 19.37° and 23.52° 2θ positions. It was found that the intensity of diffraction peaks of Kolliphor® P 188 was significantly reduced in the case of batches B4, B5 and B6. Also, the intensity of these two peaks was the lowest in batch B6 compared to batches B4 and B5. In all three batches, peaks that appeared at 2θ positions 38.29°, 44.49°, 64.75°, and 77.89° are the diffraction peaks of the sample holder, which can be ignored. Therefore, it was concluded from the results obtained using DSC and PXRD studies for the three batches that batch B6, with a processing temperature of 110 °C, was the optimum for amorphization. Furthermore, for multicomponent eutectics like RXB–MA, the polymer matrix's drug loading capacity must be increased to achieve the required potency limit. Therefore, the drug loading in the polymer matrix for batch B6 was attempted with the same processing parameters.

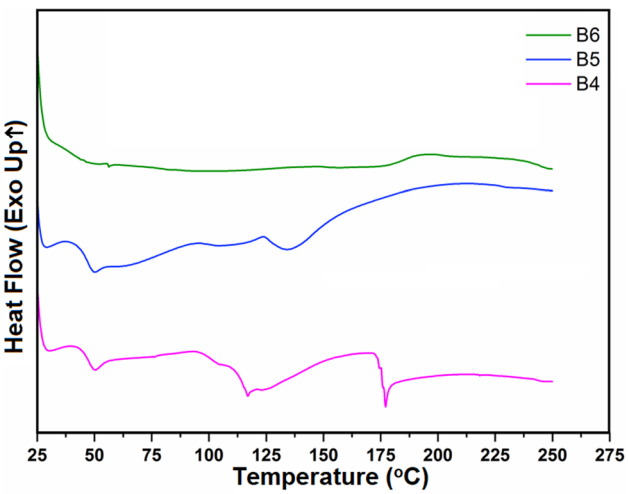

Fig. 9 DSC thermograms of B4, B5, B6, Kollidon® VA 64 and Kolliphor® P188.

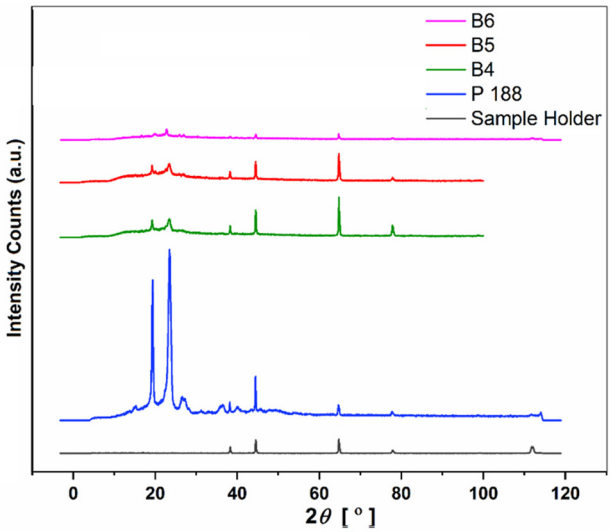

Fig. 10 PXRD diffractograms of B4, B5, B6, Kolliphor® P 188 and the sample holder.

Up to 25% eutectic could be loaded in the polymeric matrix of Kollidon® VA 64 to form a complete ASD in the presence of 5% plasticizer Kolliphor® P 188. The presence of a plasticizer can significantly improve the drug loading capacity of the polymeric matrix (ESI, Fig. S7†). Therefore, with the optimized processing conditions of batch B6, 25% eutectic was loaded and filaments were extruded.

Scanning electron microscopy (SEM)

Surface analysis of an extruded filament of B6 (25% eutectic load) was performed using the SEM technique. Horizontal (Fig. 11a) and vertical (Fig. 11b) micrographs of B6 (25% eutectic load) were analyzed. The horizontal micrograph of B6 confirmed the absence of crystalline agglomerates of RXB on the surface of the filament. The surface of B6 appeared smooth and uniform throughout its length. A small segment of the B6 filament was cut carefully and mounted vertically to observe the filament from the top. It showed that the thickness of the filament was uniform, as the top view of the filament gave a perfect circular view. Also, the absence of any crystal agglomerate or any layer suggested that RXB was completely miscible in

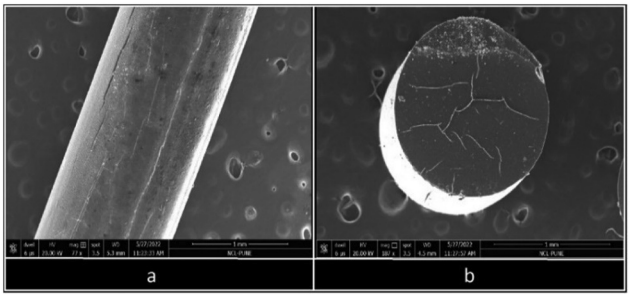

Fig. 11 SEM images of B6 (25% eutectic load): (a) horizontal surface and (b) vertical surface.

the polymeric matrix. Therefore, the vertical and horizontal sections of the B6 filament depicted the amorphous nature of the extruded filament.

Furthermore, powdered samples of RXB, the RXB–MA (1 : 4) eutectic, and the RXB–MA ASD were analyzed using SEM for particle size determination. The results reveal that RXB and the RXB–MA (1 : 4) eutectic exhibit similar particle sizes, ranging from 2 to 3 microns, characterized by sharp, defined edges. In contrast, RXB–MA ASD particles displayed a larger size, between 15 and 25 microns, with an irregular morphology lacking sharp edges (Fig. 12).

Solubility and dissolution study

RXB, the RXB–MA (1 : 4) eutectic and milled batch B6 (25% eutectic load) were stirred for 24 h and subjected to HPLC analysis. The RXB–MA (1 : 4) eutectic showed a slight improvement in the saturation solubility of RXB, whereas batch B6 showed significant enhancement in the solubility of RXB. The saturation solubility was increased by 2.989, which is approximately 3 times in the case of batch B6. Additionally, dissolution studies were performed to compare and evaluate the dissolution rates of pure RXB powder, the RXB–MA (1 : 4) eutectic, the milled and powdered batch of B6 (25% eutectic load) and the RXB marketed formulation (Xarelto™ 15 mg) (Fig. 13). The dissolution profile of these powder samples was analyzed for an hour as the marketed tablet is an immediate-release tablet.[43] RXB showed a cumulative release of 16%, whereas the RXB–MA (1 : 4) eutectic showed a very slightly enhanced cumulative release of 17%. A similar trend was observed with cocrystals of RXB with malonic acid and oxalic acid, where the dissolution rates of the cocrystals did not significantly differ from that of pure RXB.[44] On the other hand, the milled batch of B6 (25% eutectic load) showed a cumulative release of 53%, which is almost 3.3 times more than that of pure RXB powder. The dissolution profile of the RXB–MA ASD closely matched the marketed formulation, producing results nearly identical to those of the commercial product. The marketed formulation contains excipients such as croscarmellose sodium (super disintegrant), hypromellose (polymer), lactose monohydrate (diluent/filler), magnesium stearate (lubricant), microcrystalline cellulose (filler and binder), and sodium lauryl sulfate (wetting agent).[3] Remarkably, our ASD formulation did not include all of these excipients, yet it still achieved comparable dissolution performance. The addition of such excipients might further enhance the dissolution rate of our ASD formulation. An improved powder dissolution rate of RXB has been reported with the addition of surfactants like SDS (sodium dodecyl sulfate).[45]

It was also found that the dissolution of RXB in batch B6 occurred very fast within the initial 5 min as compared to the pristine drug and the eutectic. The use of MA as a coformer having more solubility than RXB and the use of hydrophilic polymer to prepare the ASD might have enhanced the dissolution rate of RXB. Also, the amorphous form of the drug shows higher dissolution rates. In ESI, Fig. S8,† the PXRD

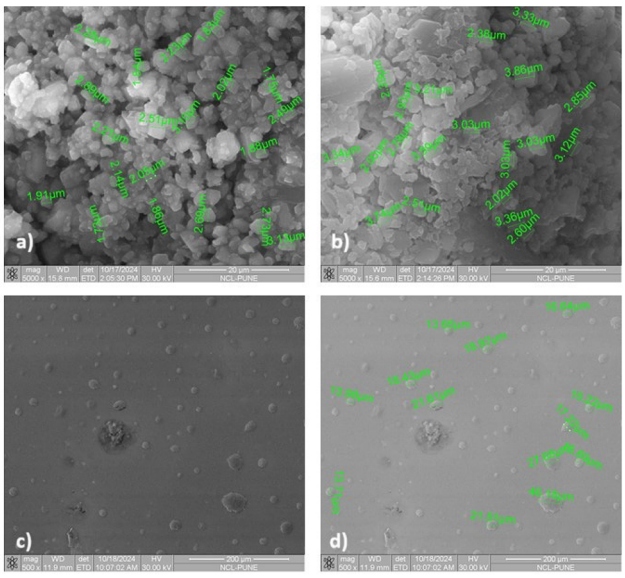

Fig. 12 SEM images of powdered samples of (a) RXB, (b) the RXB–MA (1 : 4) eutectic, (c) the RXB–MA ASD without size and (d) the RXB–MA ASD with size.

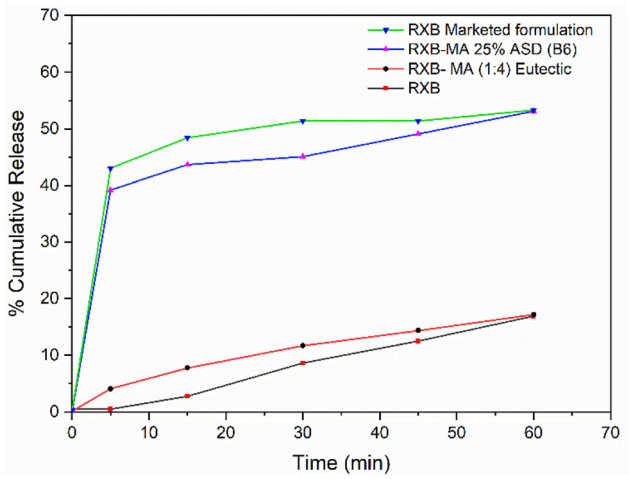

Fig. 13 The dissolution profile of RXB, the RXB–MA (1 : 4) eutectic, milled batch B6 (25% eutectic load) and RXB marketed formulation.

overlay clearly shows that the crystallinity of the RXB–MA (1 : 4) eutectic was eliminated and the final product after the HME process was amorphous.

Stability study

The stability of batch B6 (25% eutectic load) was studied under accelerated conditions for 3 months and characterized by DSC (Fig. 14) and PXRD (Fig. 15) techniques. The formulated ASD filaments were stored in glass vials. Half of the filaments were stored under open conditions and the other half were stored under closed conditions.

The DSC study showed that a small hump gradually appeared at the beginning of a thermogram from the first month to the third month. The hump might be the result of water absorption due to the hydrophilic components (Kollidon® VA 64 and Kolliphor® P 188) in the formulation. The same problem of hydrophilicity may have caused the appearance of small diffraction peaks of Kolliphor® P 188 at 2θ values of 19.37° and 23.52° in the PXRD study. High humidity under accelerated conditions for 3 months made these filaments very sticky; therefore, storing them under a dry atmosphere was recommended. However, overall, the optimized batch had no significant physicochemical change after 3 months. The PXRD results also confirmed the absence of recrystallization during the study period.

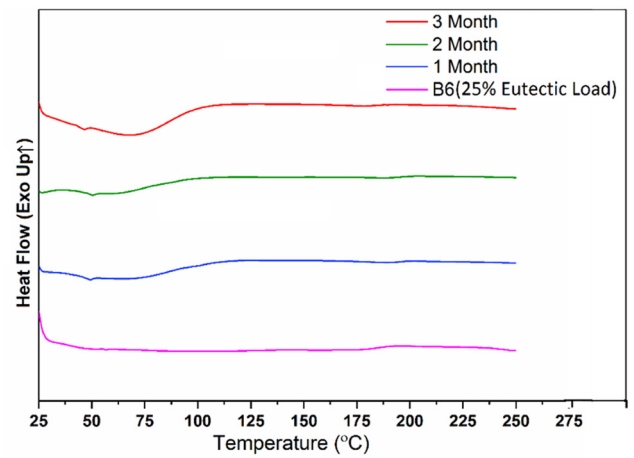

Fig. 14 DSC thermograms of B6 (25% eutectic load) and its stability for a 3-month period.

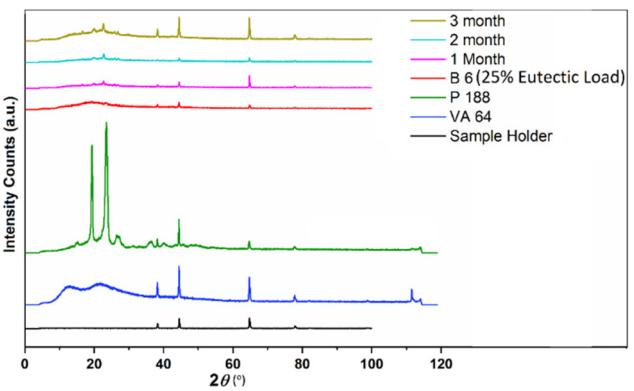

Fig. 15 PXRD of the sample holder, VA 64, P 188, and B6 (25% eutectic load) and its stability for 3 months.

Conclusions

Our study indicates that RXB degrades substantially above its melting point. Also, it was found that RXB may degrade excessively during the HME process due to prolonged exposure to heat. Therefore, to avoid the thermal degradation of RXB during the hot melt extrusion process, using the eutectic of RXB with MA in a 1 : 4 ratio was beneficial. The RXB–MA (1 : 4) eutectic melts at a lower temperature of 103.2 °C and helps reduce the processing temperature of RXB from 200 °C to 110 °C for the hot melt extrusion technique. The accelerated and long-term stability of the eutectic confirms that the eutectic was thermally stable for the entire period. Furthermore, the utilization of RXB–MA (1 : 4) in the hot melt extrusion process has significantly improved the solubility and dissolution rate of RXB by preparing an ASD with a hydrophilic polymeric matrix. Using the eutectic with a considerably lowered melting point for the HME process has improved thermal stability, solubility, and dissolution rate.

Author contributions

Rajesh G. Gonnade: conceptualization, investigation, writing – original draft, project administration, data analysis, visualization, supervision, and funding acquisition. Parth S. Shaligram, Ranjitsinh Pawar and Nagabhushan Shet: methodology, investigation, writing and editing.

Data availability

The data supporting this article have been included as part of the ESI.†

Conflicts of interest

The authors declare no competing financial interest.

Acknowledgements

P. S. S. thanks CSIR for the project fellowship under the CSIR Mission Mode Program. The help rendered by Ms Medha Ghodekar, Ms Shruti Bhavsar and Mr R. S. Gholap in carrying out the FESEM studies has been gratefully acknowledged. We gratefully acknowledge Mr Vishal Lohar for his valuable help in carrying out HME experiments. We are very thankful to Mr Ritik Balde and Ms Shital Nivdunge for their valuable help

during the revision process. This work was supported by the Science and Engineering Research Board, New Delhi (grant number EEQ/2018/001172).

References

1 T. J. Milling and S. Kaatz, *Am. J. Emerg. Med.*, 2016, **34**, 39–45.
2 T. F. Thomas, V. Ganetsky and S. A. Spinler, *Clin. Ther.*, 2013, **35**, 4–27.
3 XARELTO label information by USFDA. Available at: https://www.accessdata.fda.gov/drugsatfda_docs/label/2018/022406s028lbl.pdf.
4 D. Kubitza and S. Haas, *Expert Opin. Invest. Drugs*, 2006, **15**, 843–855.
5 C. D. Fankhauser, C. J. Sweeney and J. M. Connors, *Eur. Urol.*, 2020, **77**, 388–390.
6 Z. Xie, Y. Tian, X. Lv, X. Xiao, M. Zhan, K. Cheng, S. Li and C. Liao, *Eur. J. Med. Chem.*, 2018, **146**, 299–317.
7 C. d. C. B. Araújo, A. Simon, T. d. S. Honório, S. V. C. da Silva, I. M. M. Valle, L. C. R. P. da Silva, C. R. Rodrigues, V. P. de Sousa, L. M. Cabral, P. C. Sathler and F. A. do Carmo, *Colloids Surf., B*, 2021, **206**, 111978.
8 Md. K. Anwer, M. Mohammad, M. Iqbal, M. N. Ansari, E. Ezzeldin, F. Fatima, S. M. Alshahrani, M. F. Aldawsari, A. Alalaiwe, A. A. Alzahrani and A. M. Aldayel, *J. Thromb. Thrombolysis*, 2020, **49**, 404–412.
9 M. K. E. Sayyad, *IJRASET*, 2019, **7**, 332–342.
10 A. P. Sherje, *J. Mater. Sci.*, 2018, **29**, 186.
11 É. Sipos, G.K Lax, B. Volk, J. Barkóczy, M. Mezövári, Z. Varga and A. Dancsó, New cocrystals useful in the preparation of pharmaceutical compositions, *W.O. Pat*, WO2013054146A1, 2012.
12 A. Grunenberg, K. Fähnrich, O. Queckenberg, C. Reute, B. Keil, K. S. Gushurst and E. J. Still, Cocrystal compound of rivaroxaban and malonic acid, *United States Patent*, **20110152266**, 2011.
13 D. P. Kale, V. Puri, A. Kumar, N. Kumar and A. K. Bansal, *Pharmaceutics*, 2020, **12**, 546.
14 K. Qian, L. Stella, D. S. Jones, G. P. Andrews, H. Du and Y. Tian, *Pharmaceutics*, 2021, **13**(6), DOI: 10.3390/pharmaceutics13060889.
15 S. Cherukuvada and A. Nangia, *Chem. Commun.*, 2014, **50**, 906–923.
16 Y. Chen, G. G. Z. Zhang, J. Neilly, K. Marsh, D. Mawhinney and Y. D. Sanzgiri, *Int. J. Pharm.*, 2004, **286**, 69–80.
17 G. Z. Papageorgiou, D. Bikiaris, E. Karavas, S. Politis, A. Docoslis, Y. Park, A. Stergiou and E. Georgarakis, *AAPS J.*, 2006, **8**, 71.
18 S. Sethia and E. Squillante, *Int. J. Pharm.*, 2004, **272**, 1–10.
19 S.-C. Shin and C.-W. Cho, *Pharm. Dev. Technol.*, 1997, **2**, 403–407.
20 N. Zajc, A. Obreza, M. Bele and S. Srčič, *Int. J. Pharm.*, 2005, **291**, 51–58.
21 S. Shah, S. Maddineni, J. Lu and M. A. Repka, *Int. J. Pharm.*, 2013, **453**, 233–252.
22 S. Metre, S. Mukesh, S. K. Samal, M. Chand and A. T. Sangamwar, *Mol. Pharmaceutics*, 2018, **15**, 652–668.
23 J.-H. Lee, H. S. Jeong, J.-W. Jeong, T.-S. Koo, D.-K. Kim, Y. H. Cho and G. W. Lee, *Pharmaceutics*, 2021, **13**(3), DOI: 10.3390/pharmaceutics13030344.
24 A. Haser, S. Huang, T. Listro, D. White and F. Zhang, *Int. J. Pharm.*, 2017, **524**, 55–64.
25 S. Huang, K. P. O'Donnell, S. M. Delpon de Vaux, J. O'Brien, J. Stutzman and R. O. Williams, *Eur. J. Pharm. Biopharm.*, 2017, **119**, 56–67.
26 M.-K. Chun, K. Hossain, S.-H. Choi, S.-J. Ban, H. Moon and H.-K. Choi, *J. Pharm. Invest.*, 2012, **42**, 139–146.
27 S. Singh and J. Singh, *International Journal of Pharma and Bio Sciences*, 2010, vol. 1, ((4)), 8. Link for this article: https://www.ijpbs.net/abstract.php?article=Njk=.
28 U. Gala, H. Pham and H. Chauhan, *J. Dev. Drugs*, 2013, **2**, 1–2, DOI: 10.4172/2329-6631.1000e130.
29 P. S. Shaligram, C. P. George, H. Sharma, K. R. Mahadik, S. Patil, K. Vanka, S. Arulmozhi and R. G. Gonnade, *CrystEngComm*, 2023, **25**, 3253–3263.
30 K. Chadha, M. Karan, R. Chadha, Y. Bhalla and K. Vasisht, *J. Pharm. Sci.*, 2017, **106**, 2026–2036.
31 S. Emami, M. Siahi-Shadbad, M. Barzegar-Jalali and K. Adibkia, *J. Drug Delivery Sci. Technol.*, 2018, **45**, 101–109.
32 E. L. Charsley, P. G. Laye, H. M. Markham and T. Le Goff, *Thermochim. Acta*, 2010, **497**, 72–76.
33 J. Haneef and R. Chadha, *AAPS PharmSciTech*, 2017, **18**, 2279–2290.
34 M. Çelebier, T. Reçber, E. Koçak and S. Altinöz, *Braz. J. Pharm. Sci.*, 2013, **49**, 359–366.
35 H. Zhou, Y. Wang, S. Li and M. Lu, *Int. J. Pharm.*, 2021, **607**, 121042.
36 A. Araya-Sibaja, J. Vega-Baudrit, T. Guillén-Girón, M. Navarro-Hoyos and S. Cuffini, *Pharmaceutics*, 2019, **11**, 112.
37 D. Law, W. Wang, E. A. Schmitt, Y. Qiu, S. L. Krill and J. J. Fort, *J. Pharm. Sci.*, 2003, **92**, 505–515.
38 A. Röttele, T. Thurn-Albrecht, J.-U. Sommer and G. Reiter, *Macromolecules*, 2003, **36**, 1257–1260.
39 C. P. George, S. H. Thorat, P. S. Shaligram, P. R. Suresha and R. G. Gonnade, *CrystEngComm*, 2020, **22**, 6137–6151.
40 M. A. Repka and J. W. McGinity, *Int. J. Pharm.*, 2000, **202**, 63–70.
41 D. Desai, H. Sandhu, N. Shah, W. Malick, H. Zia, W. Phuapradit and S. R. K. Vaka, *J. Pharm. Sci.*, 2018, **107**, 372–379.
42 H. Karandikar, R. Ambardekar, A. Kelly, T. Gough and A. Paradkar, *Int. J. Pharm.*, 2015, **486**, 252–258.
43 N. R. Wingert, N. O. dos Santos, S. C. Campanharo, E. S. Simon, N. M. Volpato and M. Steppe, *Drug Dev. Ind. Pharm.*, 2018, **44**, 723–728.
44 E. Hriňová, E. Skořepová, I. Čerňa, J. Královičová, P. Kozlík, T. Křížek, J. Roušarová, P. Ryšánek, M. Šíma, O. Slanař and M. Šoóš, *Int. J. Pharm.*, 2022, **622**, 121854.
45 Y. Meng, F. Tan, J. Yao, Y. Cui, Y. Feng, Z. Li, Y. Wang, Y. Yang, W. Gong, M. Yang, X. Kong and C. Gao, *Int. J. Pharm.*, 2022, **4**, 100119.